Reconfigurable Hybrid Asymmetrical Load Modulated Balanced Amplifier with High Linearity, Wide Bandwidth, and Load Insensitivity

Jiachen Guo, Kenle Chen
Department of Electrical and Computer Engineering, University of Central Florida, USA
jiachen@knights.ucf.edu, kenle.chen@ucf.edu

2023 IEEE/MTT-S International Microwave Symposium - IMS 2023 | 979-8-3503-4764-7/23/$31.00 ©2023 IEEE | DOI: 10.1109/IMS37964.2023.10188115

***Abstract*— This paper presents the first-ever load-insensitive and highly linear three-way load-modulation power amplifier (PA) based on reconfigurable hybrid asymmetrical load modulated balanced amplifier (H-ALMBA). Through proper amplitude and phase controls, the carrier, control amplifier (CA), and two peaking balanced amplifiers (BA1 and BA2) can form a linear high-order load modulation over wide bandwidth. Moreover, it is theoretically unveiled that once CA reaches saturation at the pre-determined power back-off (PBO), its current- and voltage-source duality makes the primary (BA1) and secondary (BA2) peaking amplifiers have complementary load dependence. As such, the PA's linearity and efficiency profiles can be maintained against arbitrary load mismatch through Z_{L}-dependent reconfiguration of CA supply voltage ($V_{\mathrm{DD,CA}}$) and turning-on sequence of BA1 and BA2. Based on the proposed theory, an RF-input H-ALMBA is developed with GaN transistors and wideband quadrature hybrids. Over the design bandwidth from 1.7-2.9 GHz, an efficiency of 57%-72% at peak power and 43%-53% at 10-dB PBO are measured together with linear AMAM and AMPM responses. In modulated evaluation with 4GLTE signal, an EVM of 3.1%, ACPR of -39 dB, and average efficiency of up to 52% are measured, which are well sustained against $2:1$ VSWR of load through reconfiguration.**

***Keywords*— Balanced amplifier, high efficiency, linear, load modulation, mismatch, power amplifier, PAPR, wideband.**

I. Introduction

Spectrally efficient high-data-rate modulations have been widely adopted in emerging communications standards, which, however, greatly increases the peak-to-average power ratio (PAPR) of signals. Efficient amplification of such high-PAPR signals requires efficiency enhancement of power amplifiers (PAs) over a large output back-off (OBO) range. Besides the legacy technologies of envelope tracking (ET) and Doherty PA, many new architectures and techniques have been proposed recently, e.g., load-modulated balanced amplifiers [1], [2], offering unprecedented efficiency, OBO range, and bandwidth. However, the reported LMBAs mostly suffer from very poor linearity, thus strongly limiting their applications to systems in which digital pre-distortion is not available.

Meanwhile, massive MIMO has been widely deployed in 5G communications for expanded user capacity and higher spectrum efficiency. However, this antenna-array-based system is unavoidably subject to strong mutual couplings between antenna elements. As the direct predecessor stage of antenna, the PAs in the array are subject to a constantly varying load. To solve this challenge, multiple reconfiguration-based load-insensitive PAs are reported recently [3], [4], [5]. Nevertheless, the existing solutions are all applied to two-way load modulation, while load-insensitive three-way load-modulation PAs (ideally having larger OBO range and higher back-off efficiency) have not been practical.

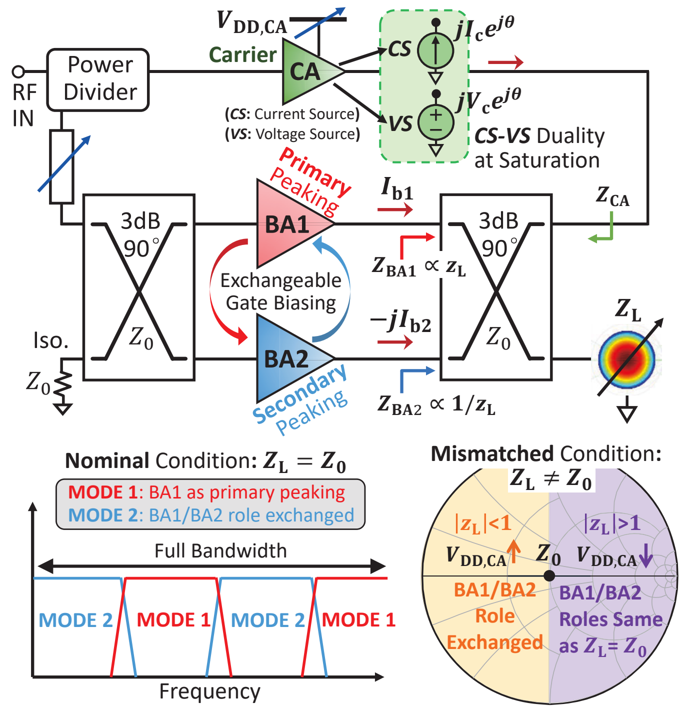

Fig. 1. Overview of H-ALMBA with varactor-less reconfiguration for wide bandwidth and load insensitiveness.

In this work, we present the first-ever linear and wideband RF-input LMBA through asymmetrical/exchangeable gate biasing of BA1 and BA2 and linearity-optimal phase control. This new H-ALMBA not only has a three-way load-modulation behavior, but it can also effectively sustain its efficiency and linearity performance against arbitrary load mismatch through z_{L}-dependent biasing reconfiguration of CA and BA. The overall conceptual schematic and its operation are illustrated in Fig. 1. Based on a rigorous theoretical analysis, the proposed concept is further experimentally validated using the developed wideband H-ALMBA prototype, demonstrating a linear and efficient performance PA performance over 1.7 – 2.9 GHz together with the desired load mismatch tolerance.

II. Theoretical Analysis of Highly Linear H-ALMBA with Load Insensitivity

Based on the H-ALMBA reported in [6], its highly linear design and mismatch resilience are analyzed in this section. As illustrated in Fig. 1, H-ALMBA is developed from the generic LMBA by setting CA as carrier, BA1 as primary peaking amplifier that turns on at deep PBO (DPBO, e.g., 10 dB), and BA2 as secondary peaking that turns on at medium PBO (MPBO, e.g., 5 dB). As a result, a three-way load modulation can be formed with multiple efficiency peaks across an extended OBO range. Through matrix analysis, the load modulation of three amplifiers can be analytically derived:

$$z_{\mathrm{CA}} = 1 - \sqrt{2}\frac{I_{b1} - I_{b2}}{I_c e^{j\theta}}, \quad (1)$$

$$z_{\mathrm{BA1}} = \frac{I_{b2}}{I_{b1}} + \frac{\sqrt{2}I_c e^{j\theta}}{I_{b1}}, \quad z_{\mathrm{BA2}} = 2 - \frac{I_{b1}}{I_{b2}} + \frac{\sqrt{2}I_c e^{j\theta}}{I_{b2}}. \quad (2)$$

where I_c, I_{b1}, and I_{b2} denote the current source of CA, BA1, and BA2, respectively, and θ the phase offset between CA and BA at the coupler plane.

A. *High-Linearity Design of H-ALMBA*

AMAM Linearization: For ideal H-ALMBA optimized for the efficiency, CA should saturate at DPBO where BA1 turns on, but this leads to a severe compression of CA and distortion of AMAM response. To solve this issue, BA1 can be turned on earlier before DPBO and load modulate with CA following above Eqs. (1) and (2) until the power reaches MPBO. Meanwhile, the turning-on of BA2 can also be earlier than MPBO in order to avoid compression. Overall, the thresholds of BA1 and BA2 can be optimized to achieve a linearized AMAM over the entire dynamic power range.

AMPM Linearization: The AMPM distortion is mainly due to the non-linear parasitic capacitors of the transistor. This can be compensated for by setting a reverse phase behavior during load modulation, which can be physically realized through properly tuning the CA-BA phase offset, θ.

B. *Reconfiguration for Resilience against Load Mismatch*

In the low-power region ($P_{\mathrm{OUT}}<P_{\mathrm{Max}}/\mathrm{OBO}$) with BA turned off, the CA load impedance (Z_{CA}) is directly converted from Z_{L} by the quadrature coupler, given by

$$z_{\mathrm{CA,LP}} = 1/z_{\mathrm{L}} = y_{\mathrm{L}}. \quad (3)$$

According to the loadline theory, the value of $V_{\mathrm{DD,CA}}$ should scale with $|z_{\mathrm{CA}}|$ in order to (approximately) maintain a voltage saturation of CA at the target DPBO, i.e., $V_{\mathrm{DD,CA}} \propto |y_{\mathrm{L}}|$. Such a load-dependent $V_{\mathrm{DD,CA}}$ can be realistically supplied by a DC-DC converter, so that the CA's dynamic efficiency and linearity profiles can be maintained against arbitrary Z_{L}.

In the high-power region ($P_{\mathrm{Max}}/\mathrm{OBO}\le P_{\mathrm{OUT}}\le P_{\mathrm{Max}}$), BA1 and BA2 are turned on sequentially and load modulated with CA. Note that that CA should remain voltage-saturated during LM, so that it can be considered as both a current source and a voltage source, i.e., CS-VS duality. We originally discovered that the z_{L}-dependence of BA1's LM behavior can only be derived by treating CA as a voltage source, given by

$$z_{\mathrm{BA1}} = \frac{\sqrt{2}V_c}{Z_0 I_{b1}} z_{\mathrm{L}} + 2z_{\mathrm{L}} - \frac{I_{b2}}{I_{b1}} \quad (4)$$

Likewise, the z_{L}-dependent LM of BA2 can only be obtained by treating CA as a current source

$$z_{\mathrm{BA2}} = \frac{\sqrt{2}I_c}{I_{b2}}\frac{1}{z_{\mathrm{L}}} + \frac{2}{z_{\mathrm{L}}} - \frac{I_{b1}}{I_{b2}}. \quad (5)$$

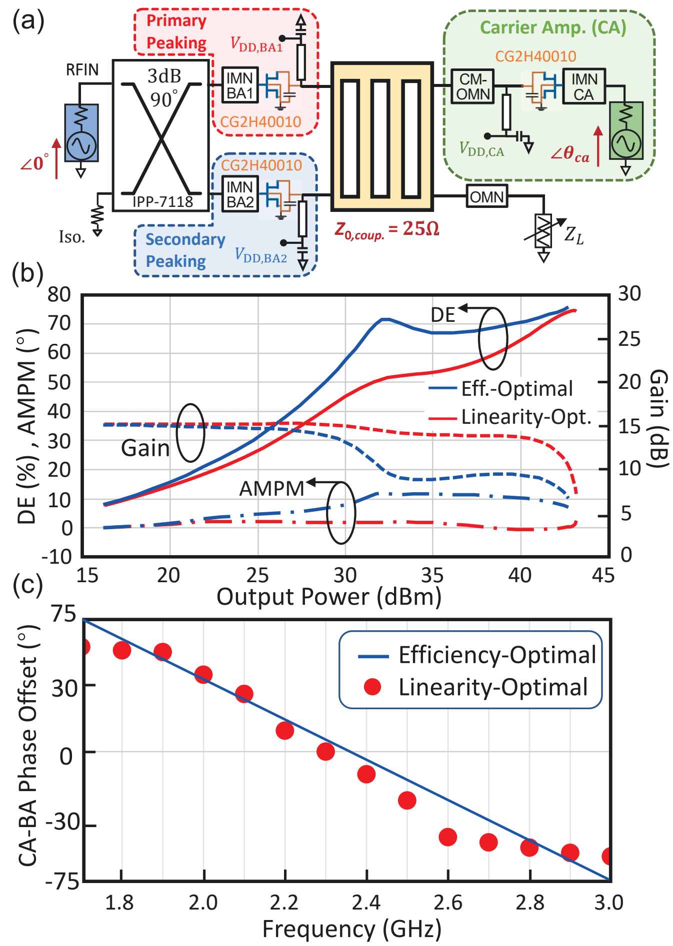

Fig. 2. Design of reconfigurable H-ALMBA: (a) circuit schematic, (b) simulated efficiency and linearity profiles, (c) determined linearity-optimal CA-BA phase offset at different frequencies.

Eqs. (4) and (5) reveal that z_{BA1} and z_{BA2} are dependent on z_{L} and $1/z_{\mathrm{L}}$, respectively, and they have symmetric math forms with respect to I_{b1} and I_{b2}. Thus, for $|z_{\mathrm{L}}| < 1$, BA1 should be the primary peaking amplifier to avoid voltage clipping during LM with CA, as depicted in Fig. 1(c). Vice versa, BA2 should be the primary peaking device for $|z_{\mathrm{L}}| > 1$. Furthermore, when BA1 and BA2 are both turned on, their operations can complement each other under load mismatch similar to a standalone balanced amplifier. As a result, a mismatch-resilient three-way LM can be formed through adjusting $V_{\mathrm{DD,CA}}$ and the turning-on sequence of BA1 and BA2.

III. Practical Design of H-ALMBA Prototype

In order to verify the proposed theory, a RF-input H-ALMBA is designed towards a target frequency range from 1.7−2.9 GHz. The 10-W GaN HEMTs (CG2H40010F) from Wolfspeed are used for both CA and BA. In order to accommodate the high PAPR of emerging 4G/5G signals, a back-off range of 10-dB is selected for this prototype.

A. *Design of Linear and Wideband RF-Input H-ALMBA*

The BA input coupler is constructed using a commercial component (IPP-7118, available from Innovative Power

Products, Inc.) with very wide bandwidth of $0.7-6$ GHz. The output coupler of BA is realized with a non-50-Ω three-stage branch hybrid structure, which can provide sufficient bandwidth and also serve as a part of output impedance matching network (OMN). The detailed design of BA and CA follow the well-sophisticated method reported in [2], [6], [7]. The designed circuit is shown in Fig. 2(a).

Fig. 2(b) shows the efficiency and linearity profiles of H-ALMBA towards different design optimum orientations. The standard H-ALMBA design [6] is optimized for efficiency where the first efficiency peak is ensured by the saturation of CA leading to a sustained high efficiency throughout the entire OBO range. However, strong distortions with $>$ 5-dB and $> 10^{\circ}$ distortions in AMAM and AMPM, respectively, are observed. Nevertheless, through the linearization techniques introduced in Sec. II-A, the AMAM and AMPM responses can be greatly flattened with slightly compromised efficiency as depicted in Fig. 2(b).

Also different from the standard LMBA or H-ALMBA design [2], [6], the linearity-optimal phase offset between CA and BA is not linearly proportional to frequency, as depicted in Fig. 2(b), which cannot be simply realized using a transmission line. Realistically, the frequency-dependent CA-BA phase offset can be realized using a tunable phase shifter. For the single RF-input design, a wideband Wilkinson divider with $1:1$ splitting ratio is designed to provide equal driving power to CA and BA.

B. Load-Mismatch-Resilient Reconfiguration

The load insensitivity of the proposed reconfigurable H-ALMBA is verified in simulation at a in-band frequency of 2.2 GHz. Under mismatch condition, the CA supply voltage ($V_{\mathrm{DD,CA}}$) and gate bias voltages of BA1 and BA2 ($V_{\mathrm{GS,BA1}}$ and $V_{\mathrm{GS,BA2}}$) are changed according to different amplitude and phase of the load VSWR. Fig. 3 shows the simulated efficiency and linearity profiles versus output power of the designed H-ALMBAprototype. Under mismatch condition, the values of $V_{\mathrm{DD,CA}}$ is adjusted to keep the first efficiency peak constantly around 10-dB as shown in Fig. 3(a), while $V_{\mathrm{GS,BA1}}$ and $V_{\mathrm{GS,BA2}}$ are optimized and/or swapped to maintain a flat AMAM and AMPM responses during load modulation as plotted in Fig. 3(b). It is demonstrated that the efficiency and linearity can both be maintained against $2:1$ VSWR with the proposed reconfiguration. This mismatch-resilient reconfiguration can be conducted at any in-band frequencies.

IV. Implementation and Experimental Results

Fig. 4 shows the measurement system setup and the photograph of the fabricated H-ALMBA. The circuit is in a size of 200 mm × 100 mm and implemented on a 20-mil thick Rogers Duroid-5880 PCB board. The PA output is connected to a standard load and a set of mismatched loads that cover the $2:1$ VSWR circle on Smith chart with the phase swept at a 30° step. The gate voltages of BA1 and BA2 are exchangeable biased from a range of -5 V to -3.4 V to maintain the overall AMAM and AMPM. The drain supply voltage of

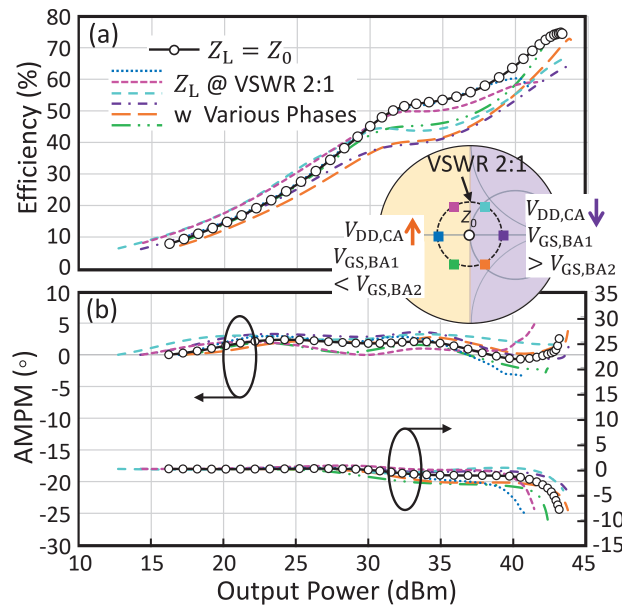

Fig. 3. Simulated H-ALMBA performance with z_{L}-optimal bias setting under various mismatch conditions: (a) efficiency, (b) linearity.

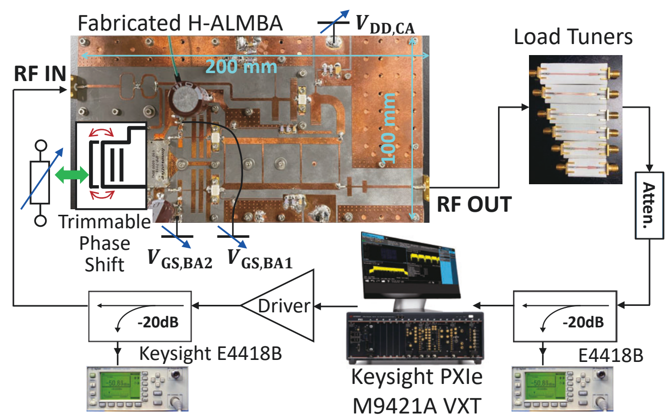

Fig. 4. Fabricated H-ALMBA with tunable parameters and testing setup.

BAs, $V_{\mathrm{DD,BA1}}$ and $V_{\mathrm{DD,BA2}}$, are identically set to 28 V to achieve their maximum output power. The CA is designed in Class-F/F^{-1} mode with a gate biasing, $V_{\mathrm{GS,CA}}$, of -2.9 V. $V_{\mathrm{DD,CA}}$ is set in an adjustable range from 7 V to 11 V to ensure its saturation is maintained at 10-dB power back-off when the load is mismatched.

The proposed prototype is first measured with a single-tone continuous-wave (CW) stimulus signal at three in-band frequencies 1.7, 2.2 and 2.6 GHz. Fig. 5 shows the frequency response of the H-ALMBA under matched contion, the proposed circuit with an optimal phase and gate biasing achieves the maximum drain efficiency (DE) of $57\%-73\%$ and 10-dB OBO DE of $43.2\%-52.8\%$ with the saturated output power of $42-43$ dBm at different frequencies. The linearity profile of H-ALMBA is flattened with a distortion of AMAM < 4.5-dB and AMPM $< 6.5^{\circ}$.

In order to validate the linearity and efficiency performance of the H-ALMBA under realistic communication, the modulated measurement is presented with a 20 MHz modulation-bandwidth single-carrier 256 QAM LTE signal.

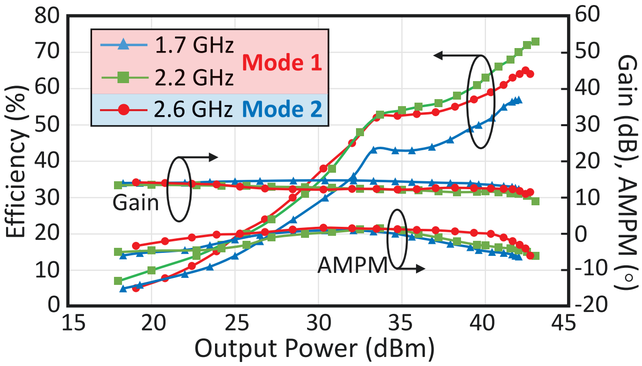

Fig. 5. Measured CW efficiency, gain and AMPM under matched condition at different frequencies.

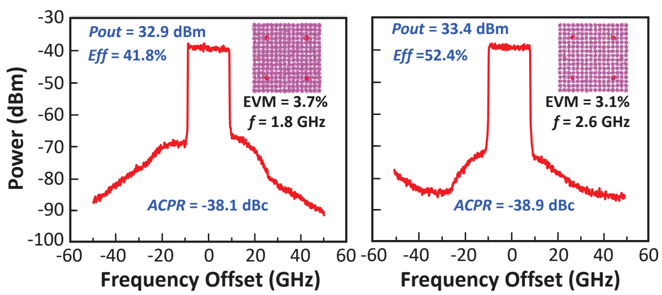

Fig. 6. Modulated measurement results using LTE signal (20 MHz, 256 QAM) under match condition at different frequencies: (a) 1.8 GHz; (b) 2.6 GHz

Fig. 6 shows the measured output spectrum at 1.8 and 2.6 GHz under matched condition with an average efficiency of $41.8\%-52.4\%$ and a best ACPR of -38.9 dBc. The PA is further measured under $2:1$ VSWR at 2.6 GHz. It is found in measurement that the linearity of H-ALMBA is devastated with load mismatch, i.e., EVM collapsed to 50% as the sample point shown in Fig. 7(a). Nevertheless, the EVM can be perfectly recovered through the proposed biasing reconfiguration. This $Z_{\rm L}$-dependent reconfiguration is conducted over the entire $2:1$ VSWR circle as shown in Fig. 7(b). A low EVM and high efficiency can both be experimentally maintained against various load conditions. The developed H-ALMBA clearly outperforms the reported Doherty PAs [5], [8], [9] in efficiency and linearity at both matched and mismatched conditions.

V. Conclusion

This paper introduces, for the first time, a wideband and linear three-way load modulation PA in H-ALMBA topology with mismatch resilience. Through theoretical analysis, the turning-on sequence of BAs in H-ALMA can be reconfigured against different load conditions due to their complementary dependence to load impedance, thus resolving the non-linearity caused by CA overdrive. Moreover, the AMPM distortion can be compensated for by tuning the CA-BA phase offset, which is in coordination with the CS-VS duality of the CA and reconfiguration by setting load-dependent voltage ($V_{\rm DD,CA}$). As a result, the overall linearity and efficiency of H-ALMBA can be maintained under arbitrary mismatched conditions. To experimentally validate the proposed theory, a prototype is developed, and the measurement results show that the designed

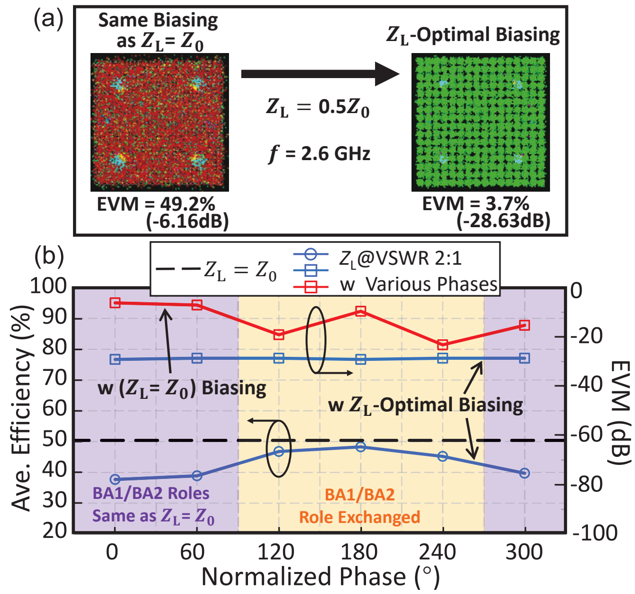

Fig. 7. Modulation measurements results across $2:1$ VSWR at 2.6 GHz with comparison between different biasing modes

H-ALMBA exhibits a highly linear performance over the bandwidth and high efficiency at both 10-dB back-off and peak power. It also well sustains the performance when transmitting modulated signal at in-band frequencies under matched load and 2:1 VSWR of load mismatch. The proposed technology can offer an effective solution of massive MIMO PA and clearly exhibits its promising potential for applications to next-generation wireless communication systems.

References

[1] D. J. Shepphard, J. Powell, and S. C. Cripps, "An efficient broadband reconfigurable power amplifier using active load modulation," *IEEE Microw. Wireless Compon. Lett.*, vol. 26, no. 6, pp. 443–445, June 2016.

[2] Y. Cao and K. Chen, "Pseudo-Doherty load-modulated balanced amplifier with wide bandwidth and extended power back-off range," *IEEE Trans. Microw. Theory Techn.*, vol. 68, no. 7, pp. 3172–3183, 2020.

[3] H. Lyu and K. Chen, "Balanced-to-Doherty mode-reconfigurable power amplifier with high efficiency and linearity against load mismatch," *IEEE Trans. Microw. Theory Techn.*, pp. 1–1, 2020.

[4] N. S. Mannem, M. Huang, T. Huang, S. Li, and H. Wang, "24.2 a reconfigurable series/parallel quadrature-coupler-based Doherty PA in CMOS SOI with VSWR resilient linearity and back-off PAE for 5G MIMO arrays," in *2020 IEEE Int. Solid-State Circuits Conf. - (ISSCC)*, 2020, pp. 364–366.

[5] H. Lyu and K. Chen, "Analysis and design of reconfigurable multiband mismatch-resilient quasi-balanced doherty power amplifier for massive mimo systems," *IEEE Transactions on Microwave Theory and Techniques*, vol. 70, no. 10, pp. 4410–4421, 2022.

[6] Y. Cao, H. Lyu, and K. Chen, "Continuous-mode hybrid asymmetrical load- modulated balanced amplifier with three-way modulation and multi-band reconfigurability," *IEEE Trans. Circuits Syst. I: Regular Papers*, pp. 1–14, 2021.

[7] J. Pang, C. Chu, Y. Li, and A. Zhu, "Broadband rf-input continuous-mode load-modulated balanced power amplifier with input phase adjustment," *IEEE Trans. Microw. Theory Techn.*, vol. 68, no. 10, pp. 4466–4478, 2020.

[8] H. Lyu, Y. Cao, and K. Chen, "Linearity-enhanced quasi-balanced doherty power amplifier with mismatch resilience through series/parallel reconfiguration for massive mimo," *IEEE Trans. Microw. Theory Techn.*, vol. 69, no. 4, pp. 2319–2335, 2021.

[9] S. Hu, F. Wang, and H. Wang, "A 28-/37-/39-GHz linear Doherty power amplifier in silicon for 5G applications," *IEEE Journal of Solid-State Circuits*, vol. 54, no. 6, pp. 1586–1599, 2019.